

CARBOXYLATED NANOCELLULOSE OBTAINED THROUGH ULTRASONICATION USING AN ALTERNATIVE ACID MIXTURE SOLVENT

JÉSSICA MICHEL DA SILVA, LUIZA RIBEIRO SANTANA, RAFAEL BELTRAME,
MÁRIO LÚCIO MOREIRA, NEFTALI LENIN VILLARREAL CARREÑO and
RAFAEL DE AVILA DELUCIS

*Postgraduate Program in Materials Science and Engineering, Federal University of Pelotas,
Pelotas, Brazil*

✉ *Corresponding authors: J. Michel da Silva, eng.jessicamichel@gmail.com
R. de Avila Delucis, rafael.delucis@ufpel.edu.br*

Received November 18, 2023

The growing concern for a safer chemical industry has spurred research towards replacing strong acid solvents, because of the significant hazards they cause, such as issues related to effluent treatment and high corrosiveness. In the production of nanocellulose, sulfuric acid stands out as an example, being highly corrosive, yet widely used. This study aimed to investigate a more ecological acid mixture solvent, specifically comprising hydrochloric acid (HCl) and citric acid (CA), for obtaining carboxylated nanocellulose from kraft cellulose pulp. Distinct methodologies were employed based on three different durations, corresponding to each methodology (30 minutes, 60 minutes, and 90 minutes). FTIR analysis confirmed the occurrence of chemical modification. Among these methodologies, ultrasonication for 60 minutes yielded the best carboxylated nanocellulose, as determined through morphological analysis, with an average diameter of 8.4 nm and an average length of 123 nm. X-ray diffraction (XRD) revealed a decrease in crystallinity; however, both kraft pulp and carboxylated nanocellulose exhibited the cellulose I β allomorph. This surface modification paves the way for incorporating new functional properties into the design of composites, hydrogels, Pickering emulsions, drug delivery systems, food packaging, and biofilms.

Keywords: nanocrystals, kraft pulp, citric acid, hydrochloric acid, carboxyl groups, carboxylation reactions

INTRODUCTION

Cellulose is characterized by its abundance, affordability, renewability, biocompatibility, and minimal impact on the food supply chain. Carboxylated nanocellulose, a well-researched class of cellulose-based nanomaterials, has traditionally been obtained through acid hydrolysis. These cellulose derivatives are produced via carboxymethylation and other carboxylation reactions, introducing carboxyl groups (-COOH) onto the cellulose polymer. This process employs reagents, such as monochloroacetic acid under alkaline conditions, enhancing water solubility.¹ Carboxylated nanocelluloses are of considerable interest due to their biodegradability, non-toxicity, renewability, and impressive mechanical properties.²⁻⁴ This biopolymer finds applications in various fields, including pharmaceuticals, food packaging, and

wastewater treatment, each requiring specific material characteristics.⁵⁻⁸

The choice of extraction techniques and processing conditions not only affects the physicochemical properties of carboxylated celluloses, but also influences their mechanical strength, thermal stability, and compatibility with other substances. Moreover, the environmental sustainability and recyclability of these solvents are crucial when designing customized solutions, aligning with the increasing demand for eco-friendly and biodegradable alternatives in various industries.²

Sulfated nanocellulose, derived from cellulose hydrolysis assisted by sulfuric acid, currently represents the most common variant among these nanomaterials. However, replacing sulfuric acid is imperative in diverse industrial and environmental

contexts. This highly corrosive acid poses significant risks to human health and the environment when mishandled or released. Transitioning from strong mineral acids, such as sulfuric acid, presents several advantages: it avoids the introduction of sulfonate groups that compromise the thermal stability of carboxylated nanocelluloses, reduces risks to personnel and equipment due to corrosiveness, and simplifies waste management and acid recycling, thereby mitigating environmental pollution.⁹

In contrast, solid acid hydrolysis conditions are gentle, less corrosive, and allow for acid reclamation. Solid acids, such as citric acid, offer a green and recyclable approach for cellulose hydrolysis to produce carboxylated nanocelluloses. However, citric acid alone may not sufficiently hydrolyze the cellulose's amorphous regions, necessitating the use of a catalyst, such as hydrochloric acid.¹⁰ Therefore, both individual acid solutions and combinations of concentrated and diluted acids, with varying acidity levels, have been explored as alternatives to strong acids, like sulfuric acid (H₂SO₄) and hydrochloric acid (HCl).¹¹ These acid solutions must meet the crucial requirement of preserving the basic cellulose backbone structure.¹²

Therefore, citric acid (CA) has emerged as a promising, greener alternative to traditional strong acid solvents in nanocellulose production, due to its environmentally friendly nature. For instance, Gomes *et al.* highlighted the potential of CA in improving enzymatic hydrolysis efficiency for sugarcane bagasse pretreatment under mild conditions.¹³ Additionally, Nagarajan *et al.* optimized CNC yield from used disposal paper cups through CA hydrolysis.¹⁴ The studies referenced above collectively underscore the efficacy and potential of CA in advancing sustainable practices in nanocellulose production and pretreatment of biomass.

Besides, previous research has shown that ultrasonic degradation of polysaccharide bonds and high-intensity ultrasonic treatment can effectively separate micro- and nanoscale carboxylated celluloses from different sources.¹⁰ The ultrasonic technique enhances the carboxylated nanocellulose yield in shorter hydrolysis times. By disrupting cellulose aggregates and facilitating the penetration of acid molecules into the inner amorphous regions, ultrasonic treatment significantly improves the hydrolysis process.¹⁵ Post-acid hydrolysis, sonication is also widely used to disperse the

produced celluloses, creating acoustic cavitation through the formation and implosive collapse of bubbles.¹⁶

The role of sonication time in the production and properties of cellulose nanocrystals has been a subject of growing interest in recent research. Guo *et al.* explored the impact of ultrasonic treatment on the structure and properties of CNCs prepared *via* acid hydrolysis, revealing that ultrasonic treatment promoted increased yields specifically for short hydrolysis times. However, it led to CNCs with shorter lengths and narrower dimension distributions due to the partial dissociation of cellulose hydrogen bond networks, resulting in delamination and disorder of the cellulose crystalline structure.¹⁷ Similarly, Pandi *et al.* employed ultrasound-assisted acid hydrolysis for synthesizing CNCs from cotton and found that the average particle size of CNCs was significantly influenced by the sonication process.¹⁸ Collectively, these studies suggest that longer sonication times typically result in smaller particle sizes and narrower size distributions, although excessive sonication can lead to material degradation and reduced yield. Therefore, optimal sonication time needs to be carefully determined for each specific application to achieve the desired properties of the final product.

Transitioning to safer and more environmentally friendly alternatives not only ensures the well-being of workers, but also reduces the ecological footprint of industrial processes. Opting for less hazardous alternatives mitigates the potential for accidents and pollution, while promoting sustainable and responsible chemical management. This research investigates a more environmentally friendly method for extracting carboxylated nanocellulose from kraft pulp, using a less aggressive acid mixture solvent and varying sonication times.

EXPERIMENTAL

Carboxylated nanocellulose extraction

All chemicals utilized in the carboxylated nanocellulose extraction were of analytical grade purity. Hydrochloric acid (HCl, 6 M) and citric acid (CA, 3 M) were sourced from Sigma-Aldrich. All chemicals and materials were stored under appropriate conditions, as recommended by the suppliers, to maintain their integrity and purity during the experimental procedures. Distilled water used throughout the process was purified using a Milli-Q water purification system, to ensure its high quality and absence of contaminants.

Carboxylated nanocellulose extraction followed the methodology of Yu *et al.*,¹⁹ with slight modifications. The process involved filtration and intermittent ultrasonic baths. Three distinct methodologies were employed, all starting with 3 grams of kraft pulp and a mixture of acids: 135 mL of 6 M hydrochloric acid (HCl) and 15 mL of 3 M citric acid (CA). Hydrolysis was conducted at 80 °C for 4 hours. After the completion of hydrolysis, the reaction solution was neutralized using a 1 M sodium hydroxide (NaOH) solution until reaching a neutral pH, monitored using a calibrated pH meter. Varying amounts of distilled water were added to the hydrolyzed pulp to achieve a consistent suspension for subsequent processing. Subsequently, the samples underwent sonication for three different durations corresponding to each methodology (30 minutes, 60 minutes, and 90 minutes). Ultrasonic treatment was conducted using an ultrasonic bath, with a frequency of 40 kHz and a power output of 100 W. The samples were then lyophilized using a freeze dryer, maintaining a temperature of -50 °C and a vacuum pressure of 0.050 mbar, to ensure complete removal of moisture and obtain dry carboxylated nanocellulose powder.

Carboxylated nanocellulose characterization

The suspended carboxylated nanocellulose samples were subjected to analysis at the Southern Electron Microscopy Center (CEME-SUL) at the Federal University of Rio Grande (FURG). A Transmission Electron Microscope (TEM), with a 120 keV capacity, specifically the Jeol, JEM-1400 model, coupled with an EDS microprobe, was used for this purpose. Origin Pro 9 software was utilized for the generation of plots and ImageJ software was employed to make measurements of fiber or particle dimensions based on the images obtained *via* TEM.

The lyophilized nanocellulose samples were analyzed at the Southern Electron Microscopy Center (CEME-SUL) at the Federal University of Rio Grande (FURG), using a D8 Advance Bruker diffractometer. The analysis was conducted at specific parameters: a scanning range from 10 to 80 degrees, at a rate of 2 degrees/min, an operating voltage of 40 kV, and a current of 40 mA. A copper (Cu) tube was utilized as the radiation source, with a wavelength (λ) of 1.5418Å, ensuring accurate and reliable X-ray diffraction measurements for characterizing the crystalline structure of the nanocellulose samples. Additionally, lyophilized nanocellulose was analyzed at the Lipidomics and Bioorganic Laboratory (LlipBio) at UFPEL, utilizing the Shimadzu IRSpirit spectrophotometer, with 45 scans spanning from 400 to 4000 cm^{-1} .

RESULTS AND DISCUSSION

Morphological analysis

The micrographs of carboxylated nanocellulose obtained after 30, 60, and 90

minutes of sonication presented distinct morphological characteristics and size distributions (see Fig. 1). The magnification level of this image is 10,000 \times . Overall, the carboxylated cellulose examined in this study exhibited dimensions within the typical ranges reported in the literature for diameter (3–70 nm) and length (70–300 nm).^{3,8} In the 30-min and 60-min sonication samples, the cellulose nanocrystals exhibited a needle-like structure, with a tendency to agglomerate in parallel. Notably, the 30-min sonication sample displayed a lower concentration of cellulose nanocrystals than the 60-min sample. This observation aligns with Salimi *et al.*,²⁰ who emphasized that sonication outcomes are influenced by factors such as cellulose concentration, processing time, and ultrasound power. In the instance of the 30-min sonication, the pronounced formation of agglomerates, coupled with reduced water content and a shorter processing time, likely influenced the unique particle characteristics observed in this suspension.

The phenomenon of agglomeration, as suggested by Kvien *et al.*,²¹ is prominent in cellulose nanocrystals. This tendency to aggregate in parallel may be attributed to the drying process during sample preparation on carbon-coated copper grids or may reflect the suspension's state. This parallel aggregation of nanocrystals has been observed in prior studies, as corroborated by our findings.

Conversely, the 90-min sonication produced spherical nanocrystals, deviating from the typical needle-like shape. According to Wang *et al.*,²² nanocellulose is characterized as amorphous and often assumes a spherical to elliptical shape, achievable through ultrasonic disintegration of regenerated cellulose solutions. The prolonged sonication, using the longest processing time, is likely the reason behind the observed shape transition.

Both the 30-min and 60-min sonication samples exhibited an increase in cellulose nanocrystal dimensions in terms of width and length. According to Naz *et al.*,²³ cellulose nanocrystals should typically fall within the width range from 4 to 70 nm and length range from 100 to 6,000 nm to qualify as such.

Notably, the results of the present study align with the work of Yu *et al.*,⁸ who successfully produced carboxylated cellulose nanocrystals (CNCs) using a mixture of citric acid and hydrochloric acid. Their CNCs exhibited lengths

and diameters of approximately 200/250 nm and 10/20 nm, respectively. Yu *et al.*¹⁹ also isolated cellulose nanocrystals from microcrystalline cellulose using a citric acid and hydrochloric acid mixture and obtained CNCs with rod-like shapes, with lengths of approximately 200–260 nm and widths of about 15–20 nm.

However, it is essential to note that the term “amorphous nanocellulose” by Ram and Chauhan²⁴ refers to materials with diameters ranging from 80 to 120 nm, a range consistent with the morphology observed in this study. Additionally, Xiong *et al.*²⁵ derived spherical cellulose nanocrystals from microcrystalline cellulose using acid hydrolysis with a nitric acid and hydrochloric acid mixture. Their obtained spherical cellulose nanocrystals primarily featured diameters ranging from 10 to 65 nm, with an average diameter of approximately 35 nm. Furthermore, Zhang *et al.*²⁶ detailed a process involving short-fiber cotton, where pre-swelling of fibers, followed by acid hydrolysis with a mixture of hydrochloric and sulfuric acid, resulted

in spherical cellulose nanocrystal particles with an average diameter of 85 nm. The cellulose particles obtained were classified as cellulose II polymorph. The studies referred to in this paragraph highlight the potential applications of materials as functional components and reinforcement in eco-friendly biocomposites.

In comparison with these studies, the 90-min sonication sample displayed larger diameters (around 100 nm), while remaining consistent with the reported literature, as many researchers have achieved much smaller sizes, well below half of the diameter observed in our sample. In summary, the 60-min sonication, which exhibited the highest quantity of cellulose nanocrystals, with dimensions in line with those reported in the literature, was selected for further characterization *via* X-ray diffraction (XRD) and Fourier-transform infrared spectroscopy (FT-IR) to validate the carboxylation of the nanocrystals and to uncover potential chemical modifications that enhance our understanding of the material and its prospective applications.

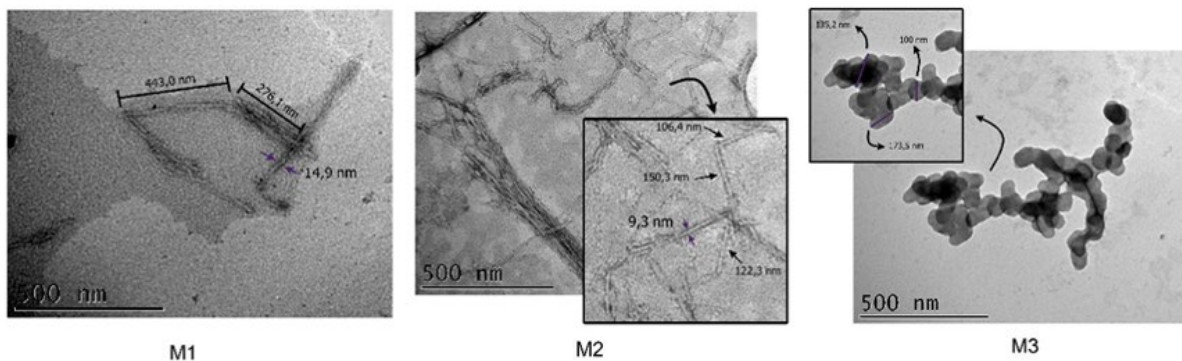


Figure 1: Transmission electron micrographs of carboxylated nanocellulose after different ultrasonication times (30, 60, and 90 minutes, respectively)

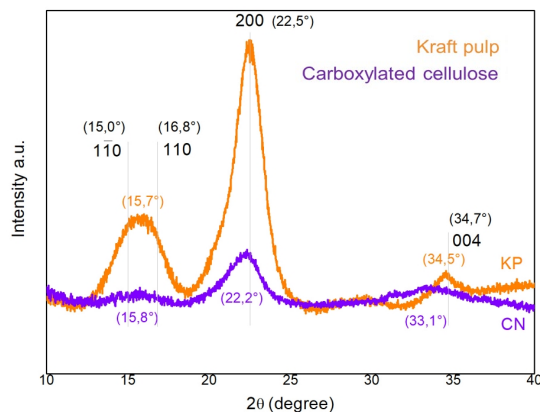


Figure 2: X-ray diffraction patterns of kraft pulp (KP) and carboxylated nanocellulose (CN)

Structural analysis

X-ray diffraction (XRD) studies of bleached pulp and nanocellulose illustrate the supramolecular structure of the kraft pulp and the lyophilized carboxylated nanocellulose (see Fig. 2). Characteristic peaks of cellulose I β were identified at $2\theta = 15.0^\circ$, 16.8° , 22.5° , and 34.7° , corresponding to Miller indices (1–10), (110), (200), and (004), as described by French.²⁷ These peaks were observed in both the kraft pulp and carboxylated nanocellulose, signifying the presence of the cellulose type I β allomorph in both materials.

Notably, the carboxylated nanocellulose displayed lower-intensity peaks compared to the kraft pulp. This observation suggests a reduction in crystallinity in the carboxylated nanocellulose samples due to the transformation process. The initial step in this process involves cellulose swelling, leading to the disruption of cellulose hydrogen bonds and increased solubility, which, in turn, results in reduced crystallinity.²⁸

This reduction in crystallinity can be attributed to the sonication process, which was described earlier. The sonication process potentially modified the crystalline structure of cellulose. Additionally, nanoscale particles often display broadened diffraction peaks due to the reduction in the size of crystalline domains, leading to the observed broadening in the peaks. Although the amorphous region and part of the crystalline region were affected, the cellulose backbone remained unaltered, maintaining its cellulose I β allomorph.

The dissolution of pulps in the system can destroy the crystallization zone due to the disruption of hydrogen bonds between cellulose macromolecules. This, in turn, reduces the crystallinity of nanocellulose and enhances the exposure of hydroxyl groups, thus improving the availability and accessibility of cellulose. This feature is essential for blending with other materials to create composites with novel properties, indicating the potential use of nanocrystals.

Chemical composition

According to the FTIR analysis, all samples exhibited normal transmittance bands of cellulose (see Fig. 3), as detailed below. The concentrated region between $3600\text{--}3200\text{ cm}^{-1}$ is related to the stretching vibrations of --OH and can be attributed to three types of intramolecular hydrogen bonds $\text{O}(2)\text{H--O}(6)$ and $\text{O}(3)\text{H--O}(5)$, as well as

intermolecular bonds $\text{O}(6)\text{H--O}(3)$.²⁹ The bands around 2900 cm^{-1} represent the symmetric stretching vibration of the --CH group.³⁰

Analyzing Figure 3 and comparing the spectra of the pulp with those of carboxylated nanocelluloses, it can be observed that the band around 3350 cm^{-1} has changed, with a new peak appearing and the band narrowing. This suggests the partial removal of amorphous regions.³¹ There is also the appearance of a new peak, which could be related to a change in intra/intermolecular hydrogen bonds. Due to the surface modification with the introduction of carboxylic groups, both intermolecular and intramolecular hydrogen bonds might be disrupted, leading to alterations in the crystalline region of carboxylated nanocellulose.³² This could indicate the decrease in crystallinity observed in the XRD analysis as well.

A hydrophilic nature is a very common characteristic of lignocellulosic materials. Water can be associated with five bands that can be analyzed in the spectra. The free hydroxyl group around 3300 cm^{-1} , demonstrating water absorption related to band intensity, experienced a decrease in this study, as mentioned above. The bound hydroxyl group around 2900 cm^{-1} , linked to carbon atoms in the cellulose structure, showed a shift and increased width between the pulp and carboxylated nanocellulose spectra. The free water band from $1600\text{--}1640\text{ cm}^{-1}$ corresponds to the H-O-H groups bending vibrations of absorbed water, which are related to the hydrophilic nature of cellulosic materials and showed no significant changes in FTIR analysis.³³ The hydroxymethyl --CH band around 1450 cm^{-1} exhibited higher intensity from pulp to carboxylated nanocellulose.³⁴ The --CO band at $1050\text{--}1150\text{ cm}^{-1}$ is related to C-O-C groups in the cellulose structure, involved in glycosidic linkages.³⁵ Upon analyzing the FTIR spectra, there was no significant change in band intensity, indicating that this chemical process kept the cellulose structure intact, without affecting it. Thus, carboxylated nanocelluloses are more hydrophilic than kraft pulp.

The peaks around 1161 cm^{-1} and 895 cm^{-1} that appear in the spectra were primarily attributed to the vibration of ether groups (C–O–C) and the oscillating vibration of --CH bonds, respectively, in the β -glycosidic linkages of the glucose ring in cellulose.³¹ A peak around 1315 cm^{-1} was also observed, attributed to the bending of the C–H bond in native cellulose, flexural vibrations in the

H–C–H and O–C–H planes.³⁶ Generally, the presence of these peaks implies that the typical native structure of cellulose was preserved throughout all stages of the isolation process.

The skeletal vibrations of the pyranose ring C–O–C are responsible for the peaks occurring around 1050 cm⁻¹.³¹ The absorption peak at 670–550 cm⁻¹ is related to -CH deformation and out-of-plane bending of -OH groups.³⁷

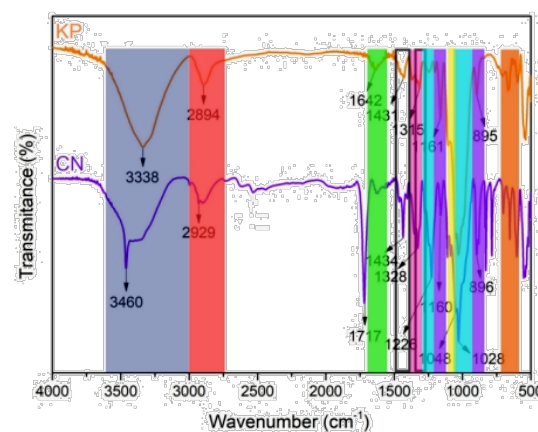
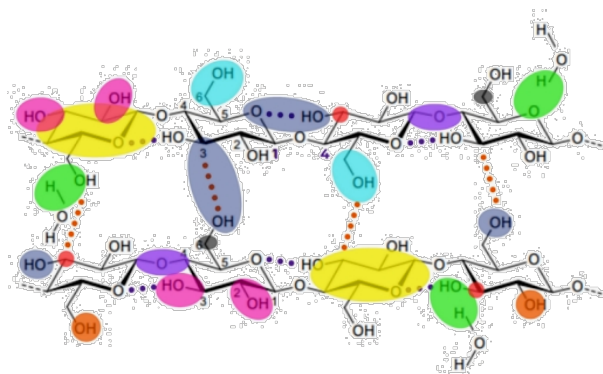


Figure 3: FTIR spectra of kraft pulp (KP) and carboxylated nanocellulose (CN)

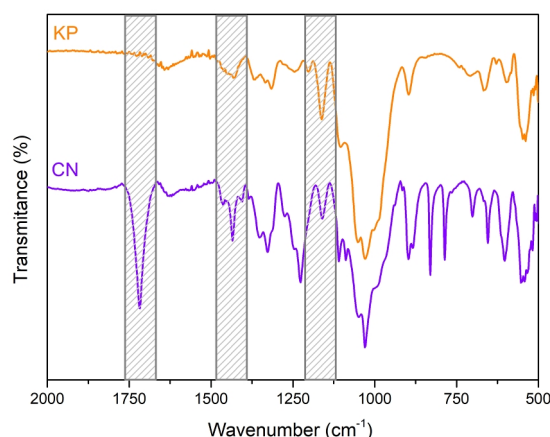


Figure 4: FTIR spectra of kraft pulp (KP) and carboxylated nanocellulose (CN) with regard to carboxylic groups

The carboxylated nanocellulose spectrum, shown in Figure 4, revealed that the chemical modifications induced various changes, including a decrease in the band associated with -OH groups at 3338 cm⁻¹ and the appearance of a new absorption band at 1717 cm⁻¹. This new band is attributed to the stretching vibration of carbonyl (C=O) groups present in the newly formed ester group. The strong peak at 1717 cm⁻¹ suggests a high degree of esterification, confirming that the carboxylated nanocellulose modified with citric acid was successfully grafted onto the carboxylated nanocellulose surfaces.⁴⁰ Other

characteristic peaks of carboxylic groups are around 1160 cm⁻¹, corresponding to the bending vibration of -OH, and 1431 cm⁻¹, corresponding to the asymmetric stretching vibration of COO-groups.⁴¹

CONCLUSION

The results of this study provide significant insights into the extraction and characterization of carboxylated nanocellulose obtained through ultrasonication using an alternative acid mixture solvent. Morphological and dimensional analysis revealed distinct shapes and size distributions in

cellulose nanocrystals and other cellulose derivatives obtained via different sonication durations. Notably, the 60-min sonication produced nanocrystals with an average diameter of 8.4 nm and a length of 123 nm, aligning with the desired nanocrystal dimensions reported in the literature.

Analysis of the crystal structure indicated a reduction in crystallinity in the carboxylated nanocellulose samples, attributed to cellulose swelling, increases in solubility and disruption of cellulose hydrogen bonds. This reduction was particularly prominent in samples subjected to longer sonication, despite both kraft pulp and carboxylated nanocellulose possessing a crystalline structure of cellulose I β allomorph.

Spectroscopic analysis of the surface of carboxylated nanocellulose revealed the introduction of carboxylic groups and the disruption of hydrogen bonds, resulting in increased hydrophilicity. The appearance of a new absorption band at 1717 cm⁻¹ suggested a high degree of esterification, confirming the successful grafting of carboxylic groups onto the cellulose surface.

In summary, these findings underscore the critical role of the sonication duration in shaping the morphological and structural properties of carboxylated nanocellulose. These outcomes provide a foundation for further research and the development of innovative materials for diverse applications.

ACKNOWLEDGEMENTS: This work was supported by the Coordination for the Improvement of Higher Education (CAPES) with Financing Code 001 and the National Council for Scientific and Technological Development (CNPq) with Financing Code 301758/2019-0.

REFERENCES

- H. Hu and F.-J. Xu, *Biomater. Sci.*, **8**, 2084 (2020), <https://doi.org/10.1039/d0bm00055h>
- K. R. Dias, B. K. Lacerda and V. Arantes, *Int. J. Biol. Macromol.*, **242**, 125053 (2023), <https://doi.org/10.1016/j.ijbiomac.2023.125053>
- M. Y. Khalid, Z. U. Arif, R. Noroozi, M. Hossain, S. Ramakrishna *et al.*, *Int. J. Biol. Macromol.*, **251**, 126287 (2023), <https://doi.org/10.1016/j.ijbiomac.2023.126287>
- R. Rinaldi and F. Schüth, *Chem. Sus. Chem.*, **2**, 1096 (2009), <https://doi.org/10.1002/cssc.200900188>
- A. Ayouch, I. Barrak, I. Kassem, Z. Kassab, K. Draoui *et al.*, *J. Environ. Chem. Eng.*, **9**, 106302 (2021), <https://doi.org/10.1016/j.jece.2021.106302>
- A. Ait Benhamou, A. Boussetta, Z. Kassab, M. Nadifiyine, H. Sehaqui *et al.*, *Constr. Build. Mater.*, **348**, 128683 (2022), <https://doi.org/10.1016/j.conbuildmat.2022.128627>
- Z. Kassab, E. Syafri, Y. Tamraoui, H. Hannache, A. E. K. Qaiss *et al.*, *Int. J. Biol. Macromol.*, **154**, 1419 (2020), <https://doi.org/10.1016/j.ijbiomac.2019.11.023>
- H. Yu, S. Y. H. Abdalkarim, H. Zhang, C. Wang and K. C. Tam, *ACS Sustain. Chem. Eng.*, **7**, 4912 (2019), <https://doi.org/10.1021/acssuschemeng.8b05526>
- E. Lam and U. D. Hemraz, *Nanomaterials*, **11**, 1641 (2021), <https://doi.org/10.3390/nano11071641>
- S. Zhu, H. Sun, T. Mu, Q. Li and A. Richel, *Food Chem.*, **403**, 134496 (2023), <https://doi.org/10.1016/j.foodchem.2022.134496>
- M. A. F. Supian, K. N. M. Amin, S. S. Jamari and S. Mohamad, *J. Environ. Chem. Eng.*, **8**, 103024 (2020), <https://doi.org/10.1016/j.jece.2019.103024>
- M. B. Noremylia, M. Z. Hassan and Z. Ismail, *Int. J. Biol. Macromol.*, **206**, 954 (2022), <https://doi.org/10.1016/j.ijbiomac.2022.03.064>
- M. G. Gomes, L. V. A. Gurgel, M. A. Baffi and D. Pasquini, *Renew. Energ.*, **157**, 332 (2020), <https://doi.org/10.1016/j.renene.2020.05.002>
- K. J. Nagarajan, A. N. Balaji, S. T. K. Rajan and N. R. Ramanujam, *Carbohydr. Polym.*, **235**, 115997 (2020), <https://doi.org/10.1016/j.carbpol.2020.115997>
- Y. Hoo, Z. L. Low, D. Y. S. Low, S. Y. Tang, S. Manickam *et al.*, *Ultrason. Sonochem.*, **90**, 106176 (2022), <https://doi.org/10.1016/j.ultsonch.2022.106176>
- P. Filson and B. Dawsonandoh, *Bioresour. Technol.*, **100**, 2259 (2009), <https://doi.org/10.1016/j.biortech.2008.09.062>
- J. Guo, X. Guo, S. Wang and Y. Yin, *Carbohydr. Polym.*, **135**, 248 (2016), <https://doi.org/10.1016/j.carbpol.2015.08.068>
- N. Pandi, S. H. Sonawane and K. A. Kishore, *Ultrason. Sonochem.*, **70**, 105353 (2021), <https://doi.org/10.1016/j.ultsonch.2020.105353>
- H.-Y. Yu, D.-Z. Zhang, F.-F. Lu and J. Yao, *ACS Sustain. Chem. Eng.*, **4**, 2632 (2016), <https://doi.org/10.1021/acssuschemeng.6b00126>
- S. Salimi, R. Sotudeh-Gharebagh, R. Zarghami, S. Y. Chan and K. H. Yuen, *ACS Sustain. Chem. Eng.*, **7**, 15800 (2019), <https://doi.org/10.1021/acssuschemeng.9b02744>
- A. Kvien, B. S. Tanem and K. Oksman, *Biomacromolecules*, **6**, 3160 (2005), <https://doi.org/10.1021/bm050479t>
- A. S. Wang, A. Lu and L. Zhang, *Prog. Polym. Sci.*, **53**, 169 (2016), <https://doi.org/10.1016/j.progpolymsci.2015.07.003>
- S. Naz, J. S. Ali and M. Zia, *Biodes. Manuf.*, **2**, 187 (2019), <https://doi.org/10.1007/s42242-019-00049-4>
- B. Ram and G. S. Chauhan, *Chem. Eng. J.*, **331**, 587 (2018), <https://doi.org/10.1016/j.cej.2017.08.128>
- R. Xiong, X. Zhang, D. Tian, Z. Zhou and C. Lu, *Cellulose*, **19**, 1189 (2012), <https://doi.org/10.1007/s10570-012-9730-4>

- ²⁶ J. Zhang, T. J. Elder, Y. Pu and A. J. Ragauskas, *Carbohydr. Polym.*, **69**, 607 (2007), <https://doi.org/10.1016/j.carbpol.2007.01.019>
- ²⁷ A. D. French, *Cellulose*, **21**, 885 (2014), <https://doi.org/10.1007/s10570-013-0030-4>
- ²⁸ M. Akhlaq and M. Uroos, *ACS Omega*, **8**, 8722 (2023), <https://doi.org/10.1021/acsomega.2c08118>
- ²⁹ G. Sèbe, F. Ham-Pichavant, E. Ibarboure, A. L. C. Koffi and P. Tingaut, *Biomacromolecules*, **13**, 570 (2012), <https://doi.org/10.1021/bm201777j>
- ³⁰ I. Mandal and D. Chakrabarty, *Carbohydr. Polym.*, **86**, 1291 (2011), <https://doi.org/10.1016/j.carbpol.2011.06.030>
- ³¹ V. Gupta, D. Ramakanth, C. Verma, P. K. Maji and K. K. Gaikwad, *Biomass Convers. Biorefin.*, **13**, 15451 (2023), <https://doi.org/10.1007/s13399-021-01852-9>
- ³² W. Wan, H. Ouyang, W. Long, W. Yan, M. He *et al.*, *ACS Sustain. Chem. Eng.*, **7**, 19202 (2019), <https://doi.org/10.1021/acssuschemeng.9b05231>
- ³³ I. F. Tarchoun, D. Trache, T. M. Klapötke, M. Derradji and W. Bessa, *Cellulose*, **26**, 7635 (2019), <https://doi.org/10.1007/s10570-019-02672-x>
- ³⁴ Chandra, S. Kumar, A. Tarafdar and P. K. Nema, *J. Sci. Food Agric.*, **101**, 2264 (2021), <https://doi.org/10.1002/jsfa.10847>
- ³⁵ W. Kamphunthong, P. Hornsby and K. Sirisinha, *J. Appl. Polym. Sci.*, **125**, 1642 (2012), <https://doi.org/10.1002/app.35642>
- ³⁶ M. A. Mohamed, W. N. W. Salleh, J. Jaafar, S. E. A. M. Asri and A. F. Ismail, *RSC Adv.*, **5**, 29842 (2015), <https://doi.org/10.1039/C4RA17020B>
- ³⁷ Q. Li and S. Rennecker, *Biomacromolecules*, **12**, 650 (2011), <https://doi.org/10.1021/bm101315y>
- ³⁸ P. Phanthong, G. Guan, Y. Ma, X. Hao and A. Abudula, *J. Taiwan Inst. Chem. Eng.*, **60**, 617 (2016), <https://doi.org/10.1016/j.jtice.2015.11.001>
- ³⁹ H. Bian, Y. Yang, P. Tu and J. Y. Chen, *Membranes*, **12**, 475 (2022), <https://doi.org/10.3390/membranes12050475>
- ⁴⁰ M. Majdoub, Y. Essamlali, O. Amadine, I. Ganetri, A. Hafnaoui *et al.*, *Cellulose*, **28**, 7717 (2021), <https://doi.org/10.1007/s10570-021-04044-w>
- ⁴¹ R. Bauli, G. F. Lima, A. G. de Souza, R. R. Ferreira and D. S. Rosa, *Colloids Surf. A Physicochem. Eng. Asp.*, **623**, 126771 (2021), <https://doi.org/10.3390/gels8090529>